Differential and total cross sections of mutual neutralization in low-energy collisions of isotopes of $H^+ + H^-$

Sifiso M. Nkambule,[*] Nils Elander,[†] and Åsa Larson[‡]
Department of Physics, Stockholm University, Albanova University Center, SE-10691 Stockholm, Sweden

Julien Lecointre[§] and Xavier Urbain[‖]
Institute of Condensed Matter and Nanosciences, Université catholique de Louvain, BE-1348 Louvain-la-Neuve, Belgium
(Received 13 October 2015; published 3 March 2016)

Mutual neutralization in the collisions of H^+ and H^- is studied both theoretically and experimentally. The quantum-mechanical *ab initio* model includes covalent states associated with the H(1)+H($n \leqslant 3$) limits and the collision energy ranges from 1 meV to 100 eV. The reaction is theoretically studied for collisions between different isotopes of the hydrogen ions. From the partial wave scattering amplitude, the differential and total cross sections are computed. The differential cross section is analyzed in terms of forward- and backward-scattering events, showing a dominance of backward scattering which can be understood by examining the phase of the scattering amplitudes for the gerade and ungerade set of states. The isotope dependence of the total cross section is compared with the one obtained using a semiclassical multistate Landau-Zener model. The final state distribution analysis emphasizes the dominance of the $n = 3$ channel for collisions below 10 eV, while at higher collision energies, the $n = 2$ channel starts to become important. For collisions of ions forming a molecular system with a larger reduced mass, the $n = 2$ channel starts to dominate at lower energies. Using a merged ion-beam apparatus, the branching ratios for mutual neutralization in H^+ and H^- collisions in the energy range from 11 to 185 eV are measured with position- and time-sensitive particle detectors. The measured and calculated branching ratios satisfactorily agree with respect to state contributions.

DOI: 10.1103/PhysRevA.93.032701

I. INTRODUCTION

When positive and negative hydrogen ions collide, charge transfer may occur, resulting in formation of neutral atoms:

$$H^- + H^+ \rightarrow H(1) + H(n), \tag{1}$$

where, at low collision energies, only one of the hydrogen atoms can be excited. This process is called mutual neutralization (MN), and it is driven by nonadiabatic interactions of electronic states, occurring at large internuclear distances. Several studies have pointed out that such a reaction will have a large cross section at low collision energies [1–10].

In the study of the formation of pregalactic clouds in the early universe, H_2 acts as a coolant [11]. Through associative detachment [12], the hydrogen anion, H^-, has been found to play a crucial role in the formation of primordial H_2 [12–18]. The MN process (1) is a competing reaction that removes H^-. Thus, for the modeling of the early universe, it is important to have reliable data with respect to the MN rate coefficient and final state distributions [13,15,16], which helps in determining the share of H^- that ends up forming H_2.

At the international ITER fusion experiment [19,20], neutral beam heating is based on an H^- (or D^-) ion source [21,22]. There is a need for modeling of the hydrogen anion density of the source. A new diagnostic technique has been suggested based on measuring the H_α/H_β Balmer line ratio [21–24]. Collisional radiative modeling shows that the measured line ratio is very sensitive to the MN rate coefficient. The MN reaction has to be studied, even for deuterium ions, since either H^- or D^- ions are produced in the ion source [20,22,25].

The first theoretical study on the MN reaction in collisions of H^+ and H^- was carried out in 1955 by Bates and Lewis [1] using a semiclassical Landau-Zener model [26,27]. Several other semiclassical studies [2,5,28–31] have followed and they all agree on a relatively large cross section that is inversely proportional to the energy and a dominance of the H(1)+H(3) channel at low collision energies. Fussen and Kubach [3] performed a quantum-mechanical study of the process using a close-coupling one-electron model. More recently, some of us [4] carried out an *ab initio* quantum-mechanical study, where the adiabatic potential energy curves and the nonadiabatic interactions were calculated using the full configuration interaction method. The coupled radial Schrödinger equation for the nuclear motion was then solved using the log-derivative method of Johnson [32].

The first experiment on this reaction was carried out by Moseley *et al.* [6] using a merged beam technique, where the total cross section was measured for relative collision energies below 3 eV. This is so far the only published measurement of the total cross section at low collision energies. At higher collision energies, however, there are other measurements of the cross section [7–10] and they more or less agree with each other and the theoretical predictions. The measured cross section by Moseley *et al.* is about a factor of 3 larger than many theoretical results and it has been debated whether the experimental cross section might be overestimated [7–10]. We have here performed measurements on MN for collisions of H^+ and H^- at intermediate energies (11–185 eV) using a

[*]sifiso.nkambule@fysik.su.se
[†]elander@fysik.su.se
[‡]aasal@fysik.su.se
[§]Present address: Haute Ecole de Namur-Liège-Luxembourg, BE-6760 Virton, Belgium; julien.lecointre@henallux.be
[‖]Xavier.Urbain@uclouvain.be

merged-beam technique. The total cross section has not been determined, but rather the final state distributions.

For the theoretical calculations, we are using the same *ab initio* quantum model for studying the process as the one by Stenrup *et al.* [4]. Electronic states of $^1\Sigma_g^+$ and $^1\Sigma_u^+$ symmetries, associated with the H(1) + H(n $\leqslant$ 3) asymptotic limits, are considered. The nonadiabatic couplings among the states, computed *ab initio* by a three-point finite difference method, are used to perform an adiabatic-to-diabatic transformation. By solving the coupled Schrödinger equation for the different partial waves, the scattering matrix elements are computed. From the matrix elements, not only the total cross section but also the differential cross section can be obtained. The total and differential cross sections as well as the final state distributions for collisions between all possible isotopes of positive and negative hydrogen ions are calculated by using the appropriate reduced mass of the system. The reaction is studied for all possible isotopes of hydrogen ions and the symmetry effects due identical nuclei and inversion symmetries are discussed.

The paper is arranged as follows. Section II discusses the formulas for the total and differential cross sections for collisions of different isotopes of hydrogen ions. In Sec. III, the merged-beam measurements are described, while in Sec. IV we present the computed differential and total cross sections as well as the comparison between measured and calculated final state distributions. A conclusion on the results can be found in Sec. V.

II. SCATTERING THEORY

Employing the full configuration interaction method with a basis set consisting of $(11s,8p,7d,2f)$ primitive Gaussian basis functions contracted to $(9s,8p,7d,2f)$, the potential energy curves and nonadiabatic interactions of the seven lowest states of $^1\Sigma_g^+$ symmetry and six lowest states of $^1\Sigma_u^+$ symmetry have been computed [4]. These are the states associated asymptotically with the H(1)+H($n \leqslant 3$) and the ion-pair, H^++H^-, limits. Using the radial first derivative nonadiabatic coupling elements, a strict adiabatic-to-diabatic transformation is performed [33]. Instead of directly solving the coupled radial Schrödinger equation, the matrix Riccati equation is solved for the logarithmic derivative of the radial wave function [32,34,35]. From the asymptotic value of the logarithmic derivative, the partial wave scattering matrix ($S_{ij,\ell}^{g/u}$) is obtained for both the gerade and ungerade manifold of states. (For more details see Ref. [4].)

For scattering of nonidentical particles (where there is no electron-inversion symmetry), the scattering amplitude is calculated from the scattering matrix as [36]

$$f_{ij}(\theta,E) = \frac{1}{2i\sqrt{k_i k_j}} \sum_\ell (2\ell+1)(S_{ij,\ell} - \delta_{ij}) P_\ell(\cos\theta). \quad (2)$$

Here k_i and k_j are the wave numbers of the final and initial states (channels), respectively, ℓ is the angular momentum quantum number, and $P_\ell(x)$ is the Legendre polynomial of degree ℓ. The differential cross section is obtained from the scattering amplitude as [36]

$$\frac{d\sigma_{ij}}{d\Omega}(\theta,E) = \frac{k_i}{k_j} |f_{ij}(\theta,E)|^2. \quad (3)$$

The total cross section is obtained by a direct integration of the differential cross section over the entire unit sphere, resulting in

$$\sigma_{ij}(E) = \frac{\pi}{k_j^2} \sum_\ell (2\ell+1)|S_{ij,\ell} - \delta_{ij}|^2. \quad (4)$$

In the present work, we study scattering of systems with two nuclei A and B which are isotopes. We study collisions $A^+ + B^-$ where the nuclear masses, m_A and m_B, may not necessarily be the same. The electronic part of the problem has inversion symmetry and the electronic states are labeled gerade (g) or ungerade (u), respectively. We can now distinguish a number of different cases caused by the colliding ions and the particular detection system of the experiment where the reaction products are measured:

(1) If the nuclear masses of the colliding ions are different ($m_A \neq m_B$), we do not have inversion symmetry but the electronic states of the collision complex can be labeled as gerade and ungerade, respectively. If we assume that we can measure the masses of the different reaction products M_A and M_B, we have one case (a), whereas if we cannot distinguish them we have another case, (b). We thus now need to formally study all cases.

(2) When ions with identical nuclei collide (A = B $\Rightarrow$ $m_A = m_B$), the overall symmetry of the total wave function of the collision complex (AB) must either be (a) antisymmetric or (b) symmetric, depending on the spin of the nuclei. When deriving the formulas of the differential cross sections for the system with total inversion symmetry, we follow the ideas of Masnou-Seeuws and Salin [37].

To formulate scattering amplitudes where the electrons are localized on one of the nuclei, the direct and exchange amplitudes are evaluated as complex-valued linear combinations of the scattering amplitudes of the gerade and ungerade states [37,38],

$$\begin{aligned} f_{ij}^{di}(\theta,E) &= \tfrac{1}{2}\left[f_{ij}^{g}(\theta,E) + f_{ij}^{u}(\theta,E)\right], \\ f_{ij}^{ex}(\theta,E) &= \tfrac{1}{2}\left[f_{ij}^{g}(\theta,E) - f_{ij}^{u}(\theta,E)\right]. \end{aligned} \quad (5)$$

For collisions of ions with *nonidentical nuclei* ($m_A \neq m_B$ such as H^++D^-), the electronic part of the Schrödinger equation still possesses the same inversion symmetry as when $m_A = m_B$. For a system with moving nuclei of different masses, the inversion symmetry is broken due to the shift between the center of mass and the center of charge [39,40]. This causes mixing between the gerade and ungerade states; however, this is neglected here.

Case 1(a). Assuming the mass of the detected atom at an angle θ is not specified, the differential cross section at this angle is obtained by incoherently adding the contributions from the direct and exchange scattering at angles θ and $\pi - \theta$, respectively [39,40]. The differential cross section becomes

$$\begin{aligned} \frac{d\sigma_{ij}}{d\Omega}(\theta,E) = {} & \frac{1}{4}\frac{k_i}{k_j}\left|f_{ij}^{g}(\theta,E) + f_{ij}^{u}(\theta,E)\right|^2 \\ & + \frac{1}{4}\frac{k_i}{k_j}\left|f_{ij}^{g}(\pi-\theta,E) - f_{ij}^{u}(\pi-\theta,E)\right|^2. \end{aligned} \quad (6)$$

The total cross section is then expressed as

$$\sigma_{ij}(E) = \frac{\pi}{2k_j^2}\sum_{\ell}(2\ell+1)\left|S^g_{ij,\ell}-\delta_{ij}\right|^2 + \frac{\pi}{2k_j^2}\sum_{\ell}(2\ell+1)\left|S^u_{ij,\ell}-\delta_{ij}\right|^2. \quad (7)$$

Note that for collisions of ions with nonidentical nuclei, the differential cross section exhibits the gerade-ungerade coherence effects, while for the total cross section all these effects are averaged out [39].

Case 1(b). If the mass of the reaction products at an angle θ can be measured separately such that one can detect if it was an atom with mass M_A or M_B that was found, the differential cross section is given by one of the two terms of Eq. (6), depending on the experimental arrangement.

Case 2(a). For collisions of ions with *identical spin*-1/2 *nuclei* (e.g., H^++H^- or T^++T^-), the overall wave function has to be antisymmetric and hence the symmetric spin function has to be combined with an antisymmetric scattering amplitude and vice versa. The symmetric and antisymmetric scattering amplitudes are calculated by linear combinations of the direct and exchange scattering amplitudes [37,39,40]. By combining the symmetrized spatial amplitudes with the corresponding spin factors, the differential cross section becomes

$$\frac{d\sigma_{ij}}{d\Omega}(\theta,E) = \frac{3}{4}\frac{k_i}{k_j}\left|f^{g,\mathrm{odd}}_{ij}(\theta,E)+f^{u,\mathrm{even}}_{ij}(\theta,E)\right|^2 + \frac{1}{4}\frac{k_i}{k_j}\left|f^{g,\mathrm{even}}_{ij}(\theta,E)+f^{u,\mathrm{odd}}_{ij}(\theta,E)\right|^2. \quad (8)$$

Here the superscript even or odd refers to a summation over even or odd angular momentum quantum numbers when the amplitudes are computed. The total cross section is again obtained by a direct integration

$$\sigma_{ij}(E) = \frac{3\pi}{4k_j^2}\sum_{\ell,\mathrm{odd}}(2\ell+1)\left|S^g_{ij,\ell}-\delta_{ij}\right|^2 + \frac{3\pi}{4k_j^2}\sum_{\ell,\mathrm{even}}(2\ell+1)\left|S^u_{ij,\ell}-\delta_{ij}\right|^2 + \frac{\pi}{4k_j^2}\sum_{\ell,\mathrm{even}}(2\ell+1)\left|S^g_{ij,\ell}-\delta_{ij}\right|^2 + \frac{\pi}{4k_j^2}\sum_{\ell,\mathrm{odd}}(2\ell+1)\left|S^u_{ij,\ell}-\delta_{ij}\right|^2, \quad (9)$$

which is the same expression as given in Ref. [4].

Case 2(b). For collisions of ions with *identical nuclei that have spin 1* (D^++D^-), the overall wave function has to be symmetric. The differential cross section becomes

$$\frac{d\sigma_{ij}}{d\Omega}(\theta,E) = \frac{k_i}{3k_j}\left|f^{g,\mathrm{odd}}_{ij}(\theta,E)+f^{u,\mathrm{even}}_{ij}(\theta,E)\right|^2 + \frac{2k_i}{3k_j}\left|f^{g,\mathrm{even}}_{ij}(\theta,E)+f^{u,\mathrm{odd}}_{ij}(\theta,E)\right|^2, \quad (10)$$

and the total cross section is given by

$$\sigma_{ij}(E) = \frac{\pi}{3k_j^2}\sum_{\ell,\mathrm{odd}}(2\ell+1)\left|S^g_{ij,\ell}-\delta_{ij}\right|^2 + \frac{\pi}{3k_j^2}\sum_{\ell,\mathrm{even}}(2\ell+1)\left|S^u_{ij,\ell}-\delta_{ij}\right|^2 + \frac{2\pi}{3k_j^2}\sum_{\ell,\mathrm{even}}(2\ell+1)\left|S^g_{ij,\ell}-\delta_{ij}\right|^2 + \frac{2\pi}{3k_j^2}\sum_{\ell,\mathrm{odd}}(2\ell+1)\left|S^u_{ij,\ell}-\delta_{ij}\right|^2. \quad (11)$$

III. EXPERIMENTAL METHOD

Using the ion-ion merged beam apparatus in operation at Université catholique de Louvain, the branching ratio among the principal quantum numbers populated by MN was determined between 11 and 185 eV. The apparatus has been described previously [41], and it is an evolution of the original setup of Szücs *et al.* [10]. The ~ 7-keV H^+ and H^- beams were extracted from an electron cyclotron resonance (ECR) and a duoplasmatron source, respectively, and merged in the ultrahigh-vacuum region of the apparatus. A 4.67-m-long drift tube and a pair of position- and time-sensitive particle detectors allow us to measure the time-of-flight (TOF) difference between hydrogen atoms resulting from MN reactions [42]. The long flight path compared to the short interaction length (7.5 cm) ensures that the small difference in exoergicity between $n = 2$ and $n = 3$ levels, i.e., 1.891 eV, shows up in the time-of-flight spectrum, as displayed in Fig. 1 for a collision energy of 58 eV.

In order to measure the TOF difference between neutral atoms in coincidence mode, we operated with inclined beams intersecting under a shallow angle of ~ 6 mrad. Each beam was pointed in such a way that all pairs of scattered atomic

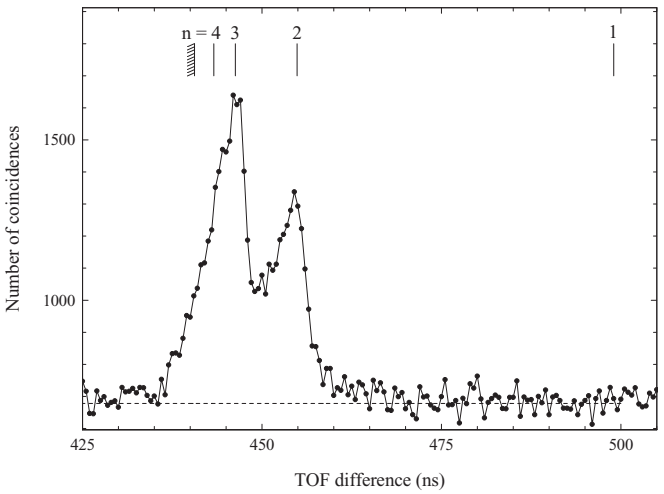

FIG. 1. Time-of-flight difference spectrum recorded at a collision energy of 58 eV (beam energies 6.1 and 7.9 keV, for H^+ and H^-, respectively) at the end of a 4.67-m-long drift tube. Numbers 1–4 on top indicate the expected time of flight for a reaction taking place in the center of the interaction region and producing H(1)+H(n) pairs.

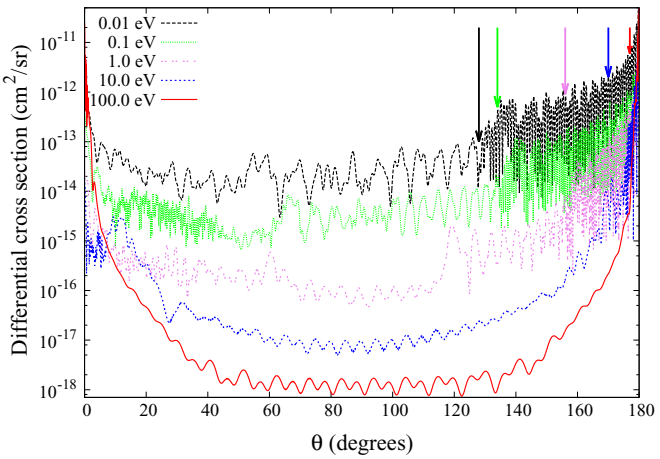

FIG. 2. Differential cross section for mutual neutralization in collisions of H^+ and H^- for selected collision energies. Arrows indicate the angles where fast oscillations start.

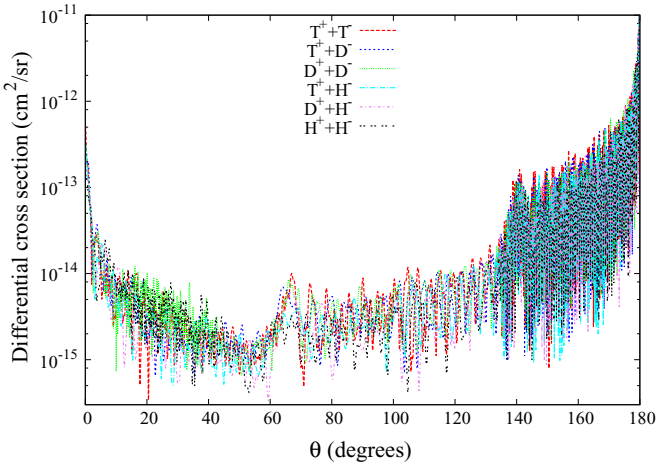

FIG. 3. Differential cross sections for mutual neutralization at 0.1 eV for collisions between different isotopes of positive and negative hydrogen ions. We here assume that the reaction products can not be distinguished.

products of the reaction fell within the geometrical acceptance of the detectors, as verified from the impact positions recorded in coincidence. A time-to-digital converter was used to build the corresponding TOF difference spectrum. Note that a full determination of the kinetic energy release is not achievable due to the imperfect collimation of the atomic beams, which prevents us from reconstructing the momentum vectors of the MN products in the center-of-mass frame. The respective contribution of each principal quantum number was extracted by a fit to the double-peak structure (see Fig. 1). No statistically significant contribution of $n > 3$ levels could be inferred from this measurement, as their contribution would fall in the leading edge of the H+H peak, whose asymmetry results from both the inclined beam geometry and the residual angular scattering in the center-of-mass frame. Furthermore, no contribution of the ground-state products is observed, which would fall at the right-hand side of the spectrum depicted in Fig. 1. This finding is discussed below in Sec. IV C.

IV. RESULTS AND DISCUSSION

A. Computed differential cross sections

The scattering amplitudes are computed and total and differential cross sections are obtained by summing up over the angular momenta, ℓ, as described in the previous section. A similar convergence criterion as in Ref. [4] is introduced to terminate the summation. The calculation of the differential cross section is carried out at a number of fixed scattering energies, and the scattering angle is varied between 0° and 180°. The total differential cross section of mutual neutralization in collisions of H^+ and H^- is presented in Fig. 2, for some selected energies. Here the contributions from all covalent states are added.

The differential cross section exhibits fast irregular oscillations as a function of the scattering angle reflecting contributions of high angular momenta. For all collision energies, the backward scattering dominates and there are even faster oscillations in the differential cross sections at large scattering angles. The arrows in Fig. 2 indicate the positions where the differential cross sections change their oscillatory behaviors. When the collision energy increases, the angle where the fast oscillations start becomes larger and the oscillations in the cross section become longer, with decreasing amplitudes, indicating a more classical motion of the particles. Additionally, as the energy increases, the cross section decreases, predominantly at $\theta = 90°$, indicating that the forward and backward scattering become more pronounced, still with a dominance of the backward scattering.

The differential cross sections are computed for mutual neutralization in collisions of all possible isotopes of the hydrogen cations and anions. The results at a collision energy of 0.1 eV are shown in Fig. 3 and it is clear that the differential cross sections are very similar for all combinations of isotopes. For collisions of ions with nonidentical nuclei the figure shows the differential cross section where the mass of the detected atom is not distinguished [using Eq. (6)]. This corresponds to case 1(a), described in Sec. II. The overall magnitudes and shapes of the differential cross sections are very similar, although the exact form of the oscillations varies. The isotope effects are very small and for all cases the backward scattering dominates and the differential cross section shows fast oscillations at large scattering angles. This does not seem to be the case for mutual neutralization of heteronuclear ions, where the molecular system has no inversion symmetry. For example, quantum-mechanical *ab initio* studies of mutual neutralization in collisions of Li^+ and H^- [43] as well as Li^+ and F^- [44] produce differential cross sections peaked at the forward direction. At small scattering angles, there are fast oscillations, and at large angles, the oscillations are slow. Using a semiclassical analysis of interfering branches of the deflection function, Delvigne and Los [45] have discussed that the angle where there is a transition between fast and slow oscillations can be understood as the Coulomb scattering angle, where the transition takes place at the distance of the closest approach. When the collision energy increases, this angle decreases.

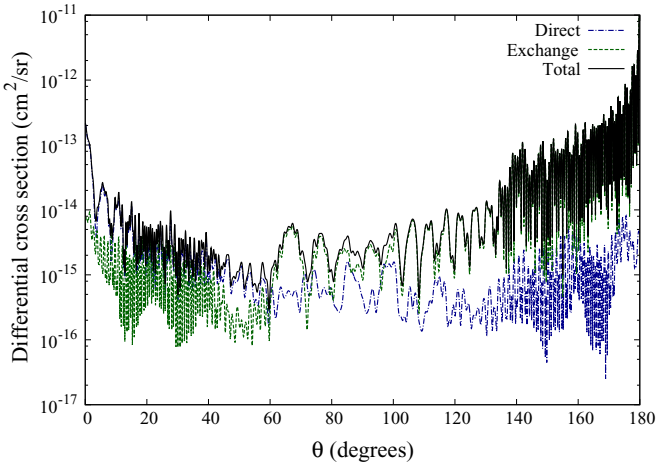

FIG. 4. Comparison of the direct and exchange contributions to the total differential cross section of the $D^+ + H^-$ system at 0.1 eV collision energy.

The present system has inversion symmetry and it is clear from Fig. 3 that the backward scattering dominates for collisions of all isotopes with the fast oscillations at large angles. The differential cross sections are computed using Eqs. (6), (8), or (10), depending on the spin of the nuclei. Since isotope effects are negligible, here we only present an analysis of the results for collisions of nonidentical nuclei, where Eq. (6) is applied. In Fig. 4, the contributions to the differential cross section from the direct and exchange scattering amplitudes are displayed for the D^+ and H^- system at 0.1 eV collision energy. It is clear that exchange scattering dominates at large angles. At $\theta \approx 60^\circ$, the direct and exchange terms switch their dominance, with the direct term having a small dominance at smaller angles. Note that these cross sections correspond to case 1(b); i.e., the masses of the products M_A and M_B are possible to distinguish in an experimental measurement.

The direct and exchange amplitudes, given by Eq. (5), are obtained as the sum (direct) and the difference (exchange) of the complex-valued gerade and ungerade scattering amplitudes, $f_{ij}^g(\theta,E) \pm f_{ij}^u(\theta,E)$. We thus need to consider both the magnitudes and the phases of these terms when computing the likewise complex-valued direct and exchange scattering amplitudes. This construction is illustrated in Fig. 5, where the matrix elements of the amplitudes for scattering to the lowest covalent state converging to the $n = 3$ limit are considered at a collision energy of 0.1 eV. For both f_{ij}^g and f_{ij}^u, the largest magnitudes are obtained at small scattering angles. For $\theta = 0^\circ$ [see Fig. 5(a)], the f_{ij}^g and f_{ij}^u are of similar magnitudes, but almost out of phase. The magnitude of the direct term, $f_{ij}^g(\theta,E) + f_{ij}^u(\theta,E)$, is thus relatively small and has approximately the same phase as f_{ij}^g. The exchange term, $f_{ij}^g(\theta,E) - f_{ij}^u(\theta,E)$, will be considerably larger than the direct scattering term and this will give rise to the large differential cross section observed in the backward direction. For $\theta = 180^\circ$, the gerade and ungerade scattering amplitudes have different magnitudes, where $|f_{ij}^g|$ is larger than $|f_{ij}^u|$. The gerade amplitude is located in the third quadrant of the complex plane while the much smaller ungerade amplitude

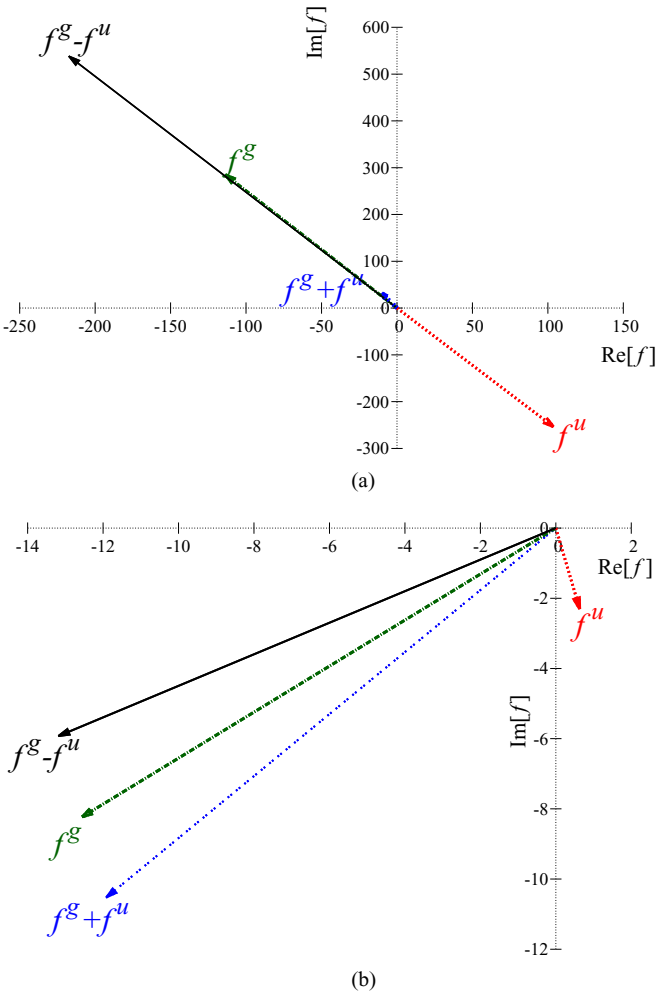

FIG. 5. The importance of the phases of f^g and f^u when forming the sums and the differences to obtain differential cross sections. (a) The sum and difference when $\theta = 0^\circ$ and (b) the results when $\theta = 180^\circ$. The procedure is discussed in the text.

is found in the fourth quadrant. Figure 5(b) illustrates the consequence: the direct and exchange amplitudes have about the same magnitudes and are both found in the third quadrant of the complex plane. This kind of analysis, when carried out for all angles and all isotope combinations, explains how the differential cross section varies with the relative collision angle as shown in Fig. 4. The large differential cross section in the backward direction can hence be understood as an interference effect due to the out-of-phase gerade and ungerade scattering amplitudes at small angles. Since inversion symmetry is not present in heteronuclear systems [43,44], the dominance of the backward scattering in the differential cross section is not likely to be found there.

B. Isotope dependence of the computed total cross section

By integrating the differential cross section, we obtain the same total cross section for MN in H^++H^- collisions as Stenrup *et al.* [4] computed directly using the scattering matrix elements [using Eq. (9)]. The total MN cross sections are computed for collisions of all hydrogen isotopes, and the

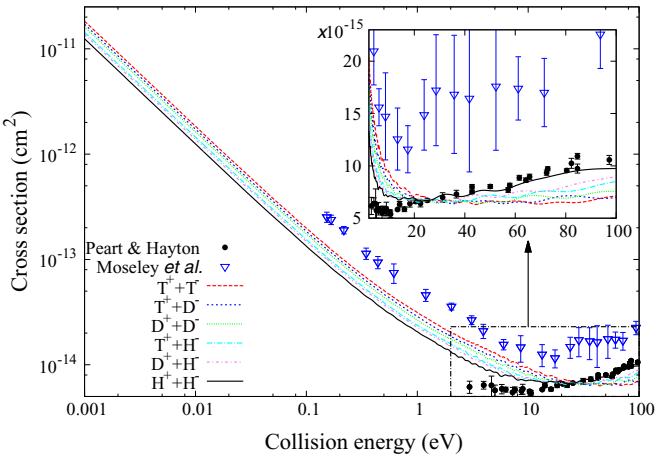

FIG. 6. Calculated total cross sections for mutual neutralization in collision of different isotopes of positive and negative hydrogen ions. The computed results are compared with measured cross sections by Peart and Hayton [7] and by Moseley *et al.* [6]. The experimental measurements are for the MN reaction of $H^+ + H^-$.

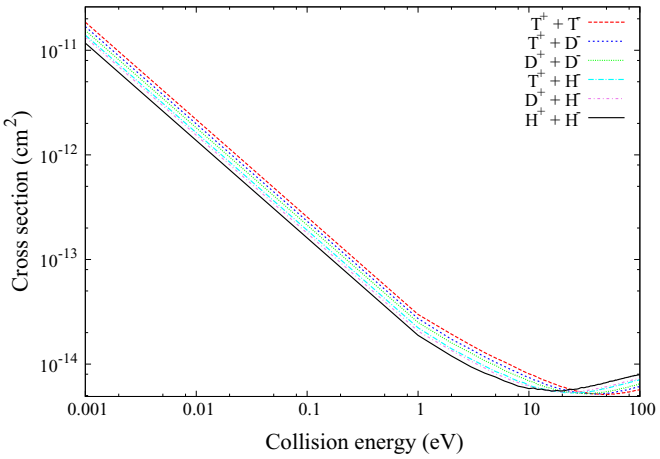

FIG. 7. Total cross section for mutual neutralization in collision of different isotopes of positive and negative hydrogen ions calculated using the Landau-Zener model.

results are presented in Fig. 6. We compare the calculated total cross section with two experimental measurements. One measurement is by Peart and Hayton [7], using a merged beam apparatus, for collisions of H^+ and H^-. The measured data cover the energy range 3–500 eV. At lower energies, the measured cross section is smaller than the cross section for $H^+ + H^-$ MN here computed, while at higher energies they are comparable. The other measurement is by Mosely *et al.* [6], who used a merged beam technique to measure the $H^+ + H^-$ MN total cross section for collision energies larger than 0.1 eV. This cross section is about a factor of 3 larger than our calculated cross section and, as pointed out previously [7–10], for the whole energy range it is larger than other results.

For collision energies approaching zero, the cross sections for all isotopes are exhibiting the E^{-1} characteristics of a Coulomb attraction [46]. The isotope dependence of the total cross section is not very large. At low energies the collision complex with larger reduced mass produces a slightly larger cross section. At 0.001 eV, the ratios of the total cross section for the heavier isotopes to that of H_2 are HD, 1.10; HT, 1.15; D_2, 1.30; DT, 1.38; and T_2, 1.47. Between 10 and 100 eV, the cross sections have a minimum and then they start to increase again. The inset of Fig. 6 shows the high-energy region where the $n = 2$ channel starts to become important. The oscillations in the cross sections are possibly quantum interference effects (Stueckelberg oscillations [47]). The position of the minimum is shifted toward larger energies with increasing reduced mass of the molecular system. A very similar isotope dependence for the present mutual neutralization reaction is obtained by carrying out a semiclassical Landau-Zener [26,27] calculation. In Fig. 7 the total mutual neutralization cross section is calculated using the multistate Landau-Zener model [5]. The electronic couplings between the ionic and covalent states are here obtained using the formula obtained by Janev [48] assuming a one-electron asymptotic method [49]. This model only considers the avoided crossings between the ionic and covalent $n = 2$ and $n = 3$ states occurring at large internuclear distances.

By comparing Figs. 6 and 7, it is clear that the relatively simple Landau-Zener model supports the isotope effects observed in the fully quantum study. At low collision energies, the system with heaviest reduced mass has the largest cross section, while it is the opposite as the energy becomes large. This isotope dependence was not observed by Croft *et al.* [43], where their *ab initio* quantal treatment of mutual neutralization in collisions of Li^+ with H^- or D^- produced a larger cross section at low energies for the lighter isotope. As the energy increases, the isotope dependence became negligible.

C. Calculated and measured final state distributions

From the scattering calculations, we also obtain information about the final state distributions in the mutual neutralization process. The present model includes all covalent $^1\Sigma_g^+$ and $^1\Sigma_u^+$ molecular states associated with the H(1)+H($n \leqslant 3$) limits. For all energies, the contribution to the H(1)+H(1) channel is very small, with a ratio to the total cross section of the order of 10^{-6}. Figure 8 presents the $n = 2$ and $n = 3$ branching ratios for mutual neutralization in collisions of different isotopes of hydrogen ions. At low collision energies the $n = 3$ channel dominates and the mutual neutralization reaction is completely driven by the avoided crossing between the ionic and covalent states at an internuclear distance of about $35a_0$. At larger energies, the avoided crossing at smaller distances can be reached and the $n = 2$ channel starts to become important. The minimum in the total neutralization cross section can be understood from the change of dominance from the $n = 3$ to the $n = 2$ dissociation channels. As can be seen, the switchover occurs at lower energies for the lighter isotopologs.

In Fig. 8, the measured branching ratios for $H^+ + H^-$ MN using the merged beam technique, described in Sec. III, are displayed. The measured final state distributions show a similar trend as the ones calculated, with a dominance of the $n = 3$ channel at low collision energies and the increasing significance of the $n = 2$ channel as the energy increases, and a complete absence of $n = 1$ contribution. At $E > 50$ eV the

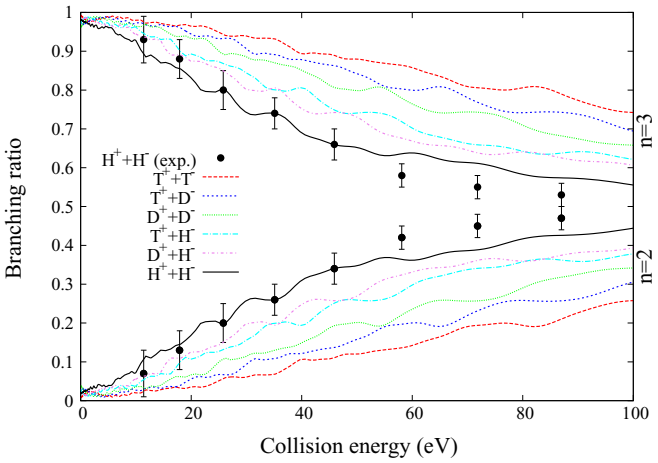

FIG. 8. Final state $n = 2$ and $n = 3$ distributions for different hydrogen isotopes, compared with experimental results for collision of H^+ and H^-.

measured $n = 2$ ratio is slightly larger than what is predicted by the theoretical calculation. At higher energies, effects not considered in the present theoretical model (such as higher electronic states, rotational couplings, or autoionization) could start to be important.

V. CONCLUSION

Mutual neutralization in low-energy H^+ and H^- collisions was studied both theoretically using a fully quantum *ab initio* model as well as experimentally using a merged beam setup. The theoretical model includes $^1\Sigma^+_{g/u}$ states associated with H(1)+H($n \leqslant 3$) channels and the reaction is studied for collisions of all possible hydrogen isotopes. The computed differential cross section exhibits fast and irregular oscillations as a function of the scattering angle. For all isotopes, there is a clear dominance of backward scattering which can be explained by the fact that the collisions cause large scattering amplitudes at small angles for the gerade and ungerade manifold of states, which are out of phase with each other. The isotope effects are studied in terms of the differential and total neutralization cross sections as well as the final state distributions. The observed dependencies of the total cross sections upon the molecular reduced mass are compared with semiclassical calculations using a multistate Landau-Zener model. The total cross section is compared with two experimental results and at higher energies, it agrees well with the cross section by Peart and Hayton [7] while it is about a factor of 3 lower than the cross section by Moseley *et al.* [6]. The measured final state distributions obtained with a merged beam apparatus show a similar form as the ones computed theoretically.

ACKNOWLEDGMENTS

We would like to thank Dr. Evgeny Yarevsky for the valuable discussions. We acknowledge support from the Swedish Research council, Grant No. 2014-4164 and the Carl Trygger foundation. J.L. and X.U. acknowledge support from the Fonds de la Rocherche Scientifique-FNRS under Contract No. 4.4504.10.

[1] D. Bates and J. Lewis, Proc. Phys. Soc. London, Sect. A **68**, 173 (1955).
[2] R. Olson, J. Peterson, and J. Moseley, J. Chem. Phys. **53**, 3391 (1970).
[3] D. Fussen and C. Kubach, J. Phys. B **19**, L31 (1986).
[4] M. Stenrup, Å. Larson, and N. Elander, Phys. Rev. A **79**, 012713 (2009).
[5] H. M. Hedberg, S. Nkambule, and Å. Larson, J. Phys. B: At. Mol. Opt. Phys. **47**, 225206 (2014).
[6] J. Moseley, W. Arbeth, and J. R. Peterson, Phys. Rev. Lett. **24**, 435 (1970).
[7] B. Peart and D. A. Hayton, J. Phys. B **25**, 5109 (1992).
[8] B. Peart, S. Foster, and K. Dolder, J. Phys. B **22**, 1035 (1989).
[9] B. Peart, M. A. Bennet, and K. Dolder, J. Phys. B **18**, L439 (1985).
[10] S. Szücs, M. Karamera, M. Terao, and F. Brouillard, J. Phys. B **17**, 1613 (1984).
[11] W. Saslaw and D. Zipoy, Nature (London) **216**, 976 (1967).
[12] K. A. Miller, H. Bruhns, J. Eliášek, M. Čížek, H. Kreckel, X. Urbain, and D. W. Savin, Phys. Rev. A **84**, 052709 (2011).
[13] S. Glover, Astrophys. J. **584**, 331 (2003).
[14] S. Glover, D. Savin, and A.-K. Jappsen, Astrophys. J. **640**, 553 (2006).
[15] S. Lepp, P. Stancil, and A. Dalgarno, J. Phys. B **35**, 0953 (2002).
[16] D. Galli and F. Palla, Astron. Astrophys. **335**, 403 (1998).
[17] E. Corbelli, D. Galli, and F. Palla, Astrophys. J. **487**, L53 (1997).
[18] H. Kreckel, H. Bruhns, M. Čížek, S. Glover, K. Miller, X. Urbain, and D. Savin, Science **329**, 69 (2010).
[19] N. Fujisawa *et al.*, Proceedings of the 18th Fusion Energy Conf., International Atomic Agency Report No. IAEA-CN-77, 2000 (unpublished).
[20] The ITER project, http://www.iter.org.
[21] U. Fantz and D. Wünderlich, New J. Phys. **8**, 301 (2006).
[22] U. Fantz, P. Franzen, W. Kraus, H. Falter, M. Berger, S. Christ-Koch, M. Fröschle, R. Gutser, B. Heinemann, C. Martens, P. McNeely, R. Reidl, E. Speth, and D. Wünderlich, Rev. Sci. Instrum. **79**, 02 (2008).
[23] U. Fantz and D. Wünderlich, AIP Conf. Proc. **1344**, 204 (2011).
[24] K. Ikeda, H. Nakano, K. Tsumori, M. Kisaki, K. Nagaoka, M. Okasabe, Y. Takeiri, and O. Kaneko, Plasma Fusion Res. Lett. **8**, 1301036 (2013).
[25] D. Wünderlich, S. Mochalskyy, U. Fantz, P. Franzen, and the NNBI Team, Plasma Sources Sci. Technol. **23**, 015008 (2014).
[26] L. Landau, Phys. Z. Sowjetunion **2**, 46 (1932).
[27] C. Zener, Proc. R. Soc. London, Ser. A **137**, 696 (1932).
[28] M. J. J. Eerden, M. C. M. van de Sanden, D. K. Otorbaev, and D. C. Schram, Phys. Rev. A **51**, 3362 (1995).
[29] A. Ermolaev, J. Phys. B: At. Mol. Opt. Phys. **21**, 81 (1988).

[30] R. Shingal and B. H. Bransden, J. Phys. B: At. Mol. Opt. Phys. **23**, 1203 (1990).
[31] V. Sidis, C. Kubach, and D. Fussen, Phys. Rev. A **27**, 2431 (1983).
[32] B. R. Johnson, Phys. Rev. A **32**, 1241 (1985).
[33] C. A. Mead and D. G. Truhlar, J. Chem. Phys. **77**, 6090 (1982).
[34] D. E. Manolopoulos, M. J. Jamieson, and A. D. Pradhan, J. Comput. Phys. **105**, 169 (1993).
[35] B. R. Johnson, J. Comput. Phys. **13**, 445 (1973).
[36] J. R. Taylor, *Scattering Theory: The Quantum Theory of Nonrelativistic Collisions* (Dover, Mineola, NY, 2006).
[37] F. Masnou-Seeuws and A. Salin, J. Phys. B **2**, 1274 (1969).
[38] L. A. Parcel and R. M. May, Proc. Phys. Soc. **91**, 54 (1967).
[39] M. P. I. Manders, W. Boom, H. C. W. Beijerinck, and B. J. Verhaar, Phys. Rev. A **39**, 5021 (1989).
[40] R. M. Jordan and P. E. Siska, J. Chem. Phys. **69**, 4634 (1978).
[41] T. Nzeyimana, E. A. Naji, X. Urbain, and A. L. Padellec, Eur. Phys. J. D **19**, 315 (2002).
[42] X. Urbain, J. Lecointre, F. Mezdari, K. A. Miller, and D. W. Savin, J. Phys. Conf. **388**, 092004 (2012).
[43] H. Croft, A. S. Dickinson, and F. X. Gadea, J. Phys. B: At. Mol. Opt. Phys. **32**, 81 (1999).
[44] S. M. Nkambule, P. Nurzia, and Å. Larson, Chem. Phys. **462**, 23 (2015).
[45] G. A. L. Delvigne and J. Los, Physica **67**, 166 (1973).
[46] E. P. Wigner, Phys. Rev. **73**, 1002 (1948).
[47] E. Stueckelberg, Helv. Phys. Acta **5**, 369 (1932).
[48] R. K. Janev, Adv. At. Mol. Phys. **12**, 1 (1976).
[49] C. Herring, Rev. Mod. Phys. **34**, 631 (1962).